Monte Carlo simulation of secondary gamma production during proton therapy for dose verification purposes

Jeyasingam Jeyasugiththan[1,2] **and Stephen Peterson**[1]

[1]Department of Physics, University of Cape Town, Rondebosch, 7701, South Africa
[2]Department of Clinical Oncology, Teaching Hospital, Jaffna, Sri Lanka

E-mail: jeyasugiththan@yahoo.com

Abstract. High energy protons can kill both cancerous as well as normal tissue, so any range uncertainty during a proton radiotherapy treatment will strongly affect the success of the overall dose delivery. In recent years, detection of prompt gammas produced by inelastic nuclear reactions between protons and nuclei within human tissue has been proposed for online treatment verification. The aim of this work is to simulate these discrete prompt gammas using the Geant4 (v9.6.02) Monte Carlo toolkit that provides several models for low energy proton inelastic nuclear reactions: binary cascade (BIC), Precompound (PRECO) and Intra nuclear cascade (INCLXX). The selection of an appropriate physics model would increase the accuracy of the prompt gamma simulations. The suitability of these models for discrete gamma emission from excited states of ^{16}O, ^{12}C and ^{14}N nuclei were tested by comparing simulated inelastic gamma production cross section data against available experimental data in the energy range 0 to 200 MeV. Among the Geant4 physics models, the Precompound model was found to be most suitable for producing reasonable prompt gamma spectra. Moreover, Fermi break up was activated below 20 MeV for complete ^{16}O simulation. A combination of different physics models in different energy regions was tested to fit a model for prompt gamma emission. Finally, a water phantom was simulated with 200 MeV proton passive beam and the prompt gamma energy spectrum was acquired by a LaBr$_3$ detector actively shielded by a BGO detector. Time-of-flight (TOF) techniques were used to eliminate scattered gammas from the beam line elements and secondary neutrons from the target. The Geant4 simulations confirmed the ability of our physics model to produce reasonable prompt gamma spectra that will be used in further studies for comparison to measured spectra.

1. Introduction

The use of x-ray photons in cancer treatment has a long history and is a well-defined method of treatment. Recent developments in radiation therapy, attacking the tumour with accelerated protons, presents unprecedented control over the dose deposition and greatly reduces the side-effects of treatment as compared to traditional x-ray radiotherapy. The proton range in a patient is uncertain for many reasons and can cause either *undershoot* to the tumour or *overshoot* to the normal tissue [1]. Although uncertainties during the calculation of the dose and patient preparation for treatment could be minimized, any range uncertainty presented during the treatment will affect the overall success of tumour control. Typically, an additional safety margin around the treatment area is applied to ensure tumour coverage [2]. This additional

margin can over-dose the normal tissue surrounding the tumour and cause serious damage to any important organs situated very close to the tumour [3], [1]. The use of a PET scanner for range verification was proposed for dose verification either immediately following treatment (on-time) or sometime after the treatment [4] [5]. Unfortunately, the treatment verification by PET/CT is seen to be insufficient at this time [5], [6]. Yet, it so far is the only available method that can be used as an *in-vivo* proton range verification device until a more precise method for online verification is developed.

A technique using prompt gamma emission from excited nuclei induced by inelastic nuclear reactions during proton radiotherapy has been attracting the attention of scientists engaged in developing a device for on-line range verification [7], [8], [9]. However, the measurement of this prompt gamma radiation in the clinical environment is still difficult due to the presence of secondary neutrons and scattered photons. In the passive beam delivery mode, additional secondary radiation activated in the beamline elements and patient final collimator is another issue. In this paper we investigate the feasibility of Geant4 Monte Carlo simulations of secondary gamma production during passive proton therapy for dose verification purposes.

2. Method
2.1. Geant4 simulations
Geant4 is an object oriented toolkit and implemented in the C++ environment [10]. It is being used to simulate the interactions of particles as they traverse through matter and is applicable in the fields of particle physics, nuclear physics, astro physics, accelerator design and medical physics. The first version of the Geant4 was released in 1998, and the following year (1999) the Geant4 collaboration was established for further development, maintenance and user support. The present work is based on the Geant4.9.6.p02 released in 2013.

Geant4 provides pre-build physics models for low energy hadronic interactions: binary cascade, precompound and intra nuclear cascade. Because of its transparency, physics models can be modified to meet user requirements by fitting of their experiment's data. In this study, the recommended reference physics list for proton radiotherapy (QGSP_BIC_EMY [11]) was used to validate the prompt gamma emissions from the elements (^{16}O, ^{12}C and ^{14}N) mostly abundant in human tissue. By default, the selected physics list provides the binary cascade model for inelastic nuclear reactions in which, the interaction is described as a two-particle binary inelastic collision between the incident proton and nucleons in the target nucleus. Further interactions between the remaining nucleons in the target nucleus and any resulting secondaries are allowed to create an intra nuclear cascade. To check the resulting secondaries, the Fermi exclusion principle is applied. If the momentum of a secondary particle falls below the Fermi level (momentum), the interaction is suppressed. Therefore the original primary particle is taken to the next interaction. On the other hand, if an interaction occurs, the secondaries are treated like primary particles. Any particle propagation into the nuclear field is determined by solving the equation of motion numerically. The cascade is terminated if the secondaries have not reached the threshold energy required for the interaction. After each interaction, particle-hole states or excitons will be added to the target nucleus and at the end of cascade, the remaining residual nuclear system with the exciton state is treated by the precompound and de-excitation models.

With respect to validations, the binary cascade model was found to underestimate the peak of the 6.13 MeV prompt gamma-ray from ^{16}O and therefore replaced by the precompound model with a modified initial exciton number of 2. The initial precompound nucleus is described by the atomic mass and charge of the residual nucleus, its four-momentum vector, its nuclear excitation energy and the number of excitons which is calculated by summing particles above the holes below Fermi level and vacant under the Fermi level of the compound nucleus. Geant4 then loops through the transitions until an equilibrium condition is reached for de-excitation which uses only the excitation energy and not the number of excitons. Several nuclear transitions are
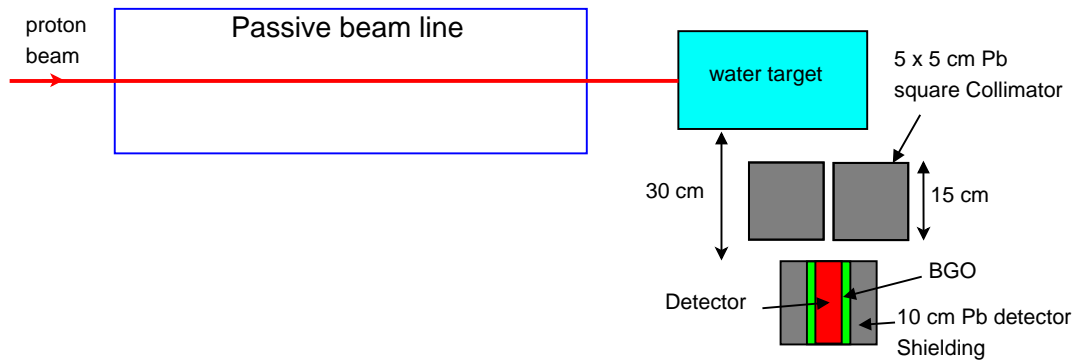
Figure 1: Simulation geometry setup with LaBr$_3$ detector.

possible with $\Delta n = \pm 2, 0$ associated with their transition probability depending on the exciton number and the excitation energy. If there is particle emission (neutrons, protons, deutrons, tritium and helium nuclei) before equilibrium is reached, the above steps are repeated with the new nuclear fragment. The particle emission is also associated with their emission probability which is a function of the exciton number and excitation energy. At statistical equilibrium, the simulation will be handled by the equilibrium model for emission of photons, nucleons and light fragments from the residual state [12]. The evaporation model is considered for the emission of nuclear fragments or gamma-rays from the excited nucleus through five different channels handled by G4ExcitationHandler: Evaporation as the main de-excitation, Fission for heavy nuclei, Fermi Break-up for light ion, Photon evaporation as competitive channel in evaporation and multifragmentation for very excited nuclei [13].

2.2. Geant4 simulation set-up

The simulation set-up is shown in the figure 1. The target is a cylindrically shaped water phantom of radius 20 cm and length 30 cm. A cylindrical LaBr$_3$ (2 inch x 2 inch) detector was surrounded by both 18 mm thick BGO ($Bi_4Ge_3O_{12}$) active shielding and 10 cm thick lead shielding, and modelled perpendicular to the beam axis with a distance between detector front face and beam axis of 30 cm. A 15 cm thick lead collimator having a 5 cm x 5 cm square hole was used to collimate the prompt gammas between the target and the detector. The previously validated Monte Carlo passive-scatter beam line model (for more details see [14]) was used to generate a 200 MeV (191 MeV at the iso-centre) proton beam of circular field with diameter of 10 cm. The modelled detector (also previously validated) was used to reproduce the detector response[14].

The purpose of the BGO active shielding was to reduce the continuous Compton background from the incomplete Compton-scattered gamma energy deposition in the LaBr$_3$ crystal using an anti-coincidence method. Also the BGO reduces the background gamma-rays produced by the neutrons hitting the lead detector shielding. The uncollimated gamma rays scattered from objects surrounding the detector were also attenuated at the lead shielding. A time-of-flight (TOF) approach was introduced in the simulation in order to reduce secondary neutrons impinging the detector from the target and scattered gamma background rays, a significant problem in passive beam radiotherapy. Inelastic nuclear reactions were simulated by using the precompound model, in which the Fermi break-up was activated for proton energy below 20 MeV.
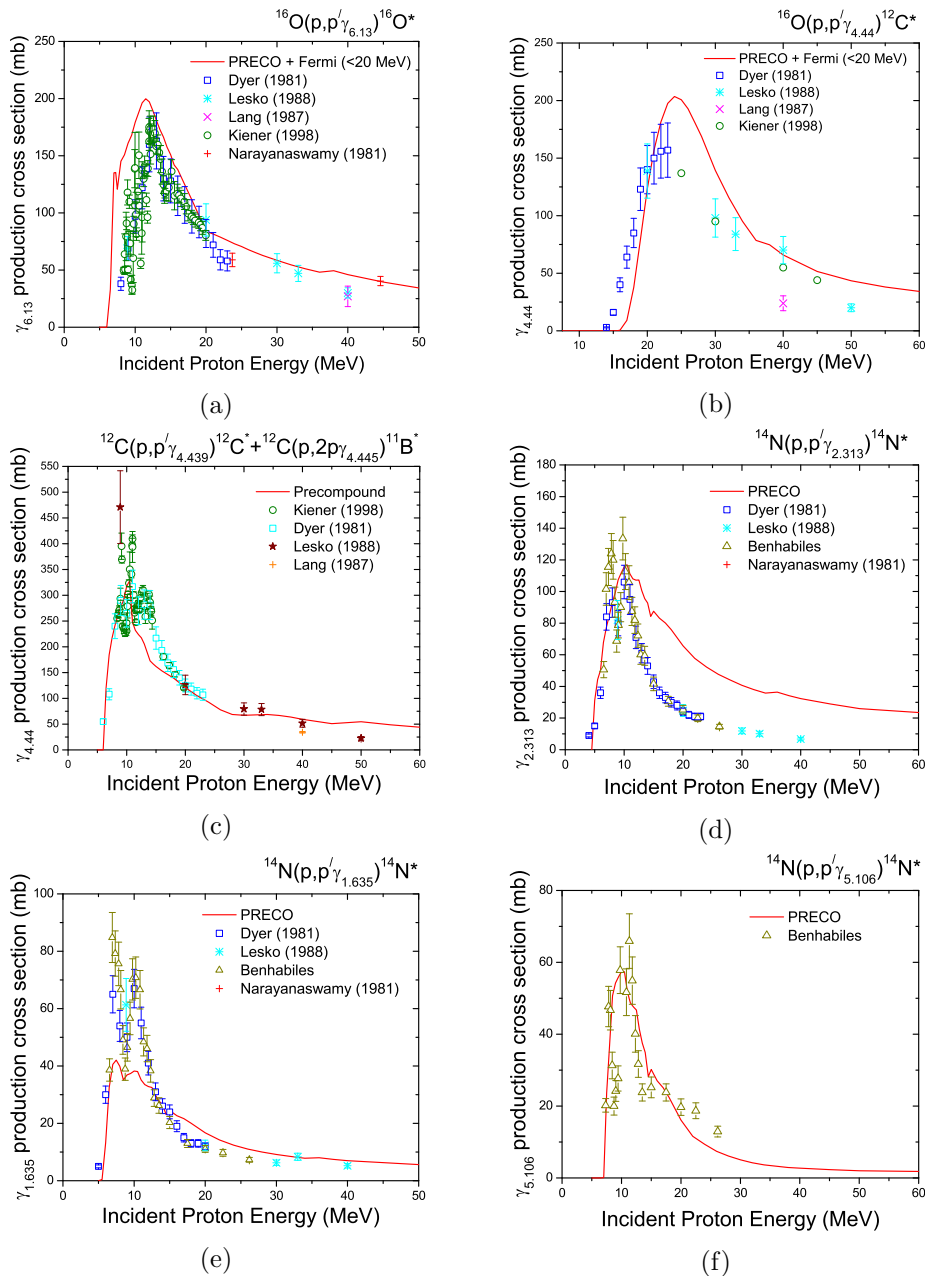
Figure 2: Comparisons between simulation and experimental cross section data for six important gamma lines produced by proton inelastic reactions on ^{16}O, ^{12}C and ^{14}N.

3. Results and Discussions

3.1. Geant4 physics validation

Figure 2 shows the comparisons between simulation and experimental cross section data currently available [15], [16], [17], [18], [19], [20] for six important gamma lines produced by proton inelastic reactions on ^{16}O, ^{12}C and ^{14}N which are the most abundant elements in human tissue. These simulations were performed using the precompound model. There were discrepancies in the gamma production performed with the default total inelastic cross sections of Willish and Axen(1996) for ^{12}C and ^{14}N. Therefore the cross sections of Tripathi et al. light ions [21] were used alternatively. The Fermi break-up below 20 MeV was required for the ^{16}O
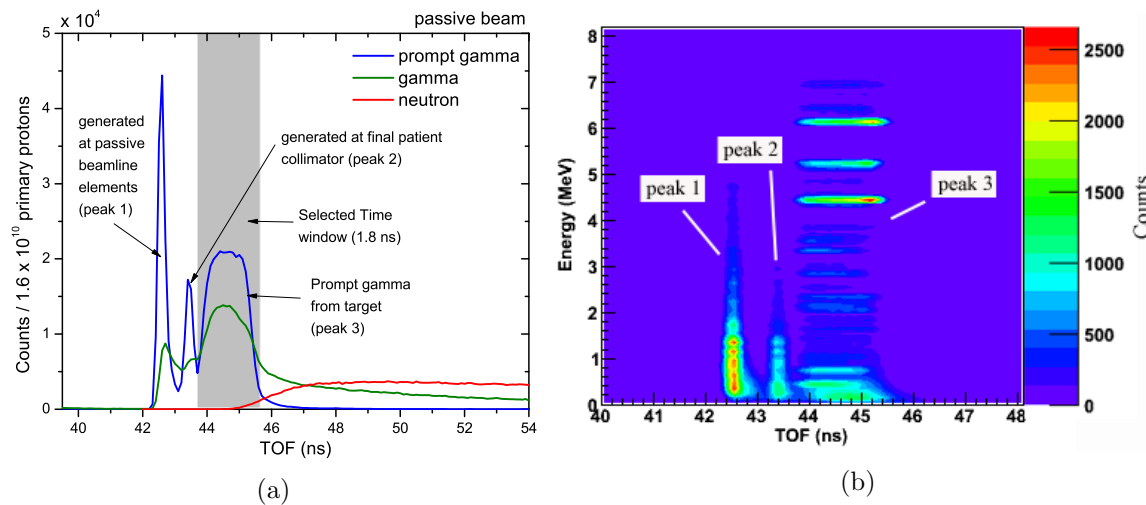
Figure 3: (a) TOF spectra of particles and (b) Time-energy spectrum of prompt gamma impinging on the LaBr$_3$ detector.
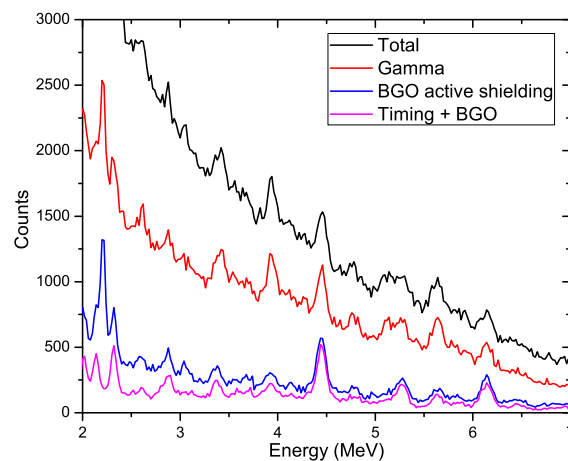

Figure 4: Comparison of energy spectra with and without background reduction methods.

simulation. Simulations of the 6.13 MeV and 4.44 MeV lines from ^{16}O, the 4.44 MeV line from ^{12}C and the 5.11 MeV line from ^{14}N all agreed well with the experimental data, unlike the other gamma-rays emitted from ^{14}N.

3.2. Geant4 simulation for prompt gamma detection

Monte Carlo time of flight (TOF) spectra are shown in figure 3a. The time of flight for the prompt gamma rays (peak 3) is shorter than slower neutrons, but greater than the scattered secondary gamma rays generated in the passive beam line elements (peak 1) and in the final patient collimator (peak 2). Therefore, a TOF window of 1.8 ns can filter out the late-arriving neutrons (about 99%) from target and as well as early-arriving background gamma rays. Moreover, the TOF window can also be coupled with an energy selection (see figure 3b). Figure 4 shows a comparison of the energy spectra simulated with and without background reduction methods applied. The simulation was carried out with 2.5 x 10^{10} incident protons entered into the passive beam line. Among them, only 8% reached the target and the remaining protons were stopped in the beamline elements and in the final collimator. The results indicate that the use of both
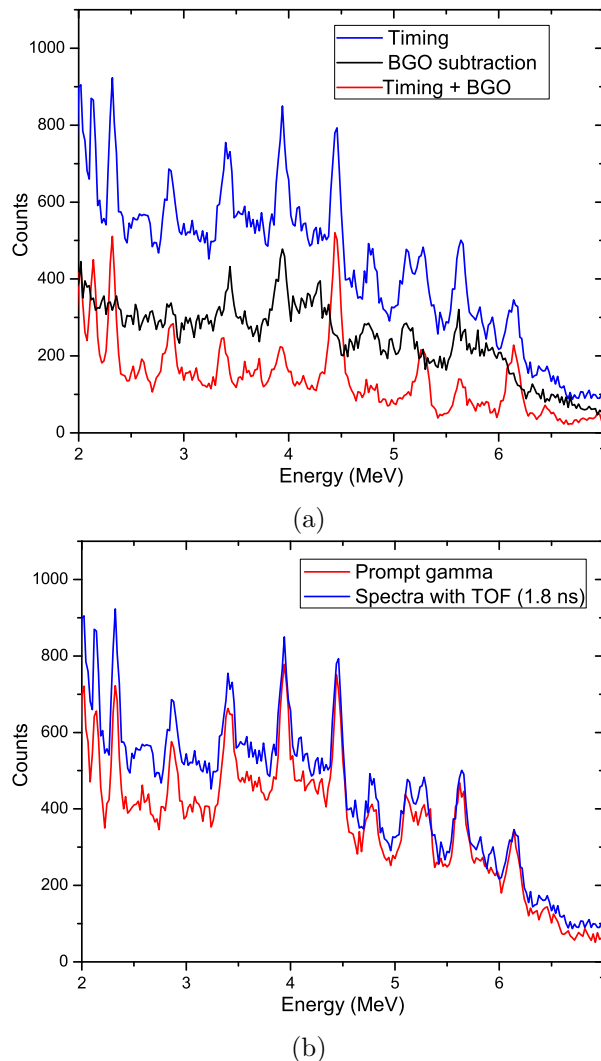
(a)

(b)

Figure 5: Comparison (a) of the energy spectra using a 1.8 ns TOF window (with and without BGO active shielding) and (b) of the energy spectra of the prompt gammas produced within the target to the TOF spectra from the LaBr$_3$ detector.

timing and active shielding is able to remove 90% of the background radiation which includes a 10% reduction due to BGO subtraction as shown in figure 5a. Peaks at 6.13, 4.44 and 5.24 MeV from $^{16}O^*$, $^{12}C^*$ and $^{15}O^*$ respectively are clearly identified when both timing and BGO subtraction are used. Subtraction of Compton-scattered background is required to resolve the 5.24 MeV peak from the second escape peak of 6.13 MeV. Comparison between the prompt gamma spectra detected from the target and the spectra using the TOF window shown in figure 5b is promising, showing a prompt gamma detection with an efficiency of 72.4%.

4. Conclusion

Our study confirmed the feasibility of Geant4 simulation for prompt gamma-rays in the passive-scatter proton beam mode. The background reduction using a TOF window was excellent. Also BGO subtraction helped to resolve the prompt gamma peaks from Compton background. The physics model is able to reproduce the prompt gamma spectra that will be used in our further studies for comparison to measured data.

Acknowledgments

The authors would like to thank the Center for High Performance Computing (CHPC), CSIR Campus, 15 Lower Hope St., Rosebank, Cape Town, in South Africa for providing them access to their computing resources.

References

[1] Lu H M 2008 *Physics in Medicine and Biology* **53** N415
[2] Paganetti H 2002 *Physics in Medicine and Biology* **47** 747
[3] Trofimov A, Nguyen P L, Coen J J, Doppke K P, Schneider R J, Adams J A, Bortfeld T R, Zietman A L, DeLaney T F and Shipley W U 2007 *International Journal of Radiation Oncology*Biology*Physics* **69** 444 – 453 ISSN 0360-3016
[4] Maccabee H D, Madhvanath U and Raju M R 1969 *Phys. Med. Biol.* **14** 213–24
[5] Parodi K, Bortfeld T and Haberer T 2008 *International Journal of Radiation Oncology*Biology*Physics* **71** 945 – 956 ISSN 0360-3016
[6] Knopf A, Parodi K, Bortfeld T, Shih H A and Paganetti H 2009 *Physics in Medicine and Biology* **54** 4477
[7] Min C, Kim C H, Youn M and Kim J 2006 *Appl. Phys. Lett.* **89** 183517
[8] Polf J C, Peterson S, Ciangaru G, Gillin M and Beddar S 2009a *Phys. Med. Biol.* **54** 731
[9] Verburg J M, Riley K, Bortfeld T and Seco J 2013 *Physics in Medicine and Biology* **58** L37
[10] Agostinelli S, Allison J, Amako K and Apostolakis J 2003 *Nuclear Instruments and Methods in Physics Research Section A: Accelerators, Spectrometers, Detectors and Associated Equipment* **506** 250 – 303 ISSN 0168-9002
[11] Cirrone G A P, Cuttone G, Mazzaglia S E, Romano F, Sardina D, Agodi C, Attili A, Blancato A A, Napoli M D, Rosa F D, Kaitaniemi P, Marchett F, Petrovic I, Ristic-Fira A, Shin J, Tarnavsky N, Tropea S and Zacharatou C 2011 *Progress in nuclear science and technology* **2** 207–212
[12] Jarlskog C Z and Paganetti H 2008 *IEEE Trans. Nucl. Sci.* **55** 1018–1025
[13] Lara V and Wellisch J P 2000 *9th Int. Conf. Calorimetry in High Energy Physics* 449–452
[14] Jeyasugiththan J, Peterson S, Camero J N and Symons J 2014 *Proceedings of the 58th Annual Conference of the South African Institute of Physics, edited by Roelf Botha and Thulani Jili* **pp. 260-267** ISBN: 978–0–620–62819–8. Available online at http://events.saip.org.za
[15] Dyer P, Bodansky D, Seamster A G, Norman E B and Maxson D R 1981 *Phys. Rev. C* **23** 1865–82
[16] Lesko K T, Norman E B, Larimer R M, Kuhn S, Meekhof D M, Crane S G and Bussell H G 1988 *Phys. Rev. C* **37**(5) 1808–1817
[17] Lang F L, Werntz C W, Crannell C J, Trombka J I and Chang C C 1987 *Phys. Rev. C* **35** 1214–27
[18] Kiener J, Berheide M, Achouri N L, Boughrara A, Coc A, Lefebvre A, de Oliveira Santos F and Vieu C 1998 *Phys. Rev. C* **58**(4) 2174–2179
[19] Narayanaswamy J, Dyer P, Faber S R and Austin S M 1981 *Phys. Rev. C* **24** 2727–30
[20] Benhabiles-Mezhoud H, Kiener J, Thibaud J P, Tatischeff V, Deloncle I, Coc A, Duprat J, Hamadache C, Lefebvre-Schuhl A, Dalouzy J C, de Grancey F, de Oliveira F, Dayras F, de Séréville N, Pellegriti M G, Lamia L and Ouichaoui S 2011 *Phys. Rev. C* **83**(2) 024603
[21] Tripathi R K, Cucinotta F A and Wilson J W 1999 *Technical Report TP-1999-209726 National Aeronautics and Space Administration (NASA)*